Biofidelity Evaluation of a Restrained Whole Body Finite Element Model under Frontal Impact using Kinematics Data from PMHS Sled Tests

[1]Mike W.J. Arun, John R. Humm, Narayan Yoganandan, Frank A. Pintar

Abstract The present study evaluated the kinematics of the Global Human Body Model Consortium (GHBMC) model, under frontal impact. Resultant acceleration data from simulations at head center of gravity (CG), T1, sternum, T12, and sacrum were compared with sled test responses. The objectives of the present study were to normalize the experimental data, qualitatively compare the simulation kinematics to that of the PMHS response, and quantify the goodness-of-fit using correlation analyses (CORA). Kinematics data from restrained eight PMHS tests – low (3.3 m/s), and medium (6.7 m/s) – were used to evaluate the biofidelity of the GHMBC model under frontal impact. The experimental data were normalized to represent 50th percentile male population, to minimize response variations due to demographics. The restrained GHBMC model was positioned with its standard posture on a rigid seat. Simulations were performed using two different input speeds – low, and medium - under frontal impact conditions. Qualitative observation of the kinematics between simulations and experiments indicated a good match. CORA ratings ranged from 0.51 to 0.78, and 0.53 to 0.75 for the low, and medium speed cases respectively, indicating acceptable kinematic biofidelity of the model under frontal impact.

Keywords Finite element model, GHBMC, Validation, Biofidelity, Frontal impact.

I. INTRODUCTION

Delineating injury mechanisms in impact biomechanics is critical to prevent or attenuate injury-causing factors through counter-measures. Traditionally, this delineation is done using post mortem human specimens (PMHS) [1, 2], computer models [3], and anthropometric test devices (ATD, also known as "dummies") [4, 5]. However, compared to real life humans, the stiffness and biofidelity of these devices are very different, as they are designed for repeated testing. Computer models constructed using rigid bodies, were available for crash investigations since early 1960's [6], however these models were limited in their capabilities, mainly due to the lack, and cost of computational hardware at that time. Several finite element (FE) based human body models (HBM) were recently developed due to the exponential increase in cost-efficient powerful computational hardware [7, 8]. In addition, rigorously formulated FE explicit theories [9, 10], and solvers – like Ls-Dyna, Pam-Crash etc., - accelerated the developments of these detailed FE models. Nevertheless, in order to obtain trustworthy data from these HBMs, they must be validated against PMHS tests, for different modes, and rates of loadings. Anthropometric variations are unavoidable in PMHS experiments. Generally, these variations influence experimental responses [11]. To minimize these variations, individual PMHS responses can be normalized to a predetermined reference population, such as mid-sized male [12-14], to be used to validate HBMs.

One such detailed FE HBM was created – by the Global Human Body Model Consortium (GHBMC) - to represent 50th percentile American male, with a standard seating posture. The GHBMC HBM was built with 1.95 million elements, and 1.3 million nodes to represent a detailed anatomical geometry of the whole body parts. Past studies have evaluated various biofidelity aspects of the model, under different modes, and rates of impact loading. Park *et al.* (2013) evaluated the biofidelity of the model under lateral impact, using kinematics data from sled tests. The model was impacted laterally with a rigid impactor to validate responses to that of PMHS responses [15]. Hayes *et al.* (2014) used chestband data to validate the thoracic response of the GHBMC model,

Mike W.J. Arun (marun@mcw.edu) is a Post-Doctoral Fellow, John R. Humm is a Research Engineer, Narayan Yoganandan is a Professor, Frank A. Pintar is a Professor, in the Department of Neurosurgery at Medical College of Wisconsin in the United States of America.

under frontal, and lateral impact conditions [16]. Vavalle *et al.* (2015) used region specific data from the model to validate the biofidelity of chest, shoulder, thorax, and abdominal responses [17]. However, the kinematics of the head, and spine has not been validated for the whole GHBMC model under frontal impact. Because kinematics could directly influences kinetics – for example, accelerations directly influence forces – therefore, evaluating the kinematics of the model, using PMHS data may be a crucial step to ensure the reliability of the model. The present study evaluated the kinematics of the GHBMC model, under frontal impact. Resultant acceleration data from simulations at head center of gravity (CG), T1, sternum, T12, and sacrum were compared with sled test responses. The objectives of the present study were to normalize the experimental data, qualitatively compare the simulation kinematics to that of the PMHS response, and quantify the goodness-of-fit using correlation analyses (CORA).

II. METHODS

Experimental setup:

Restrained (three-point belt and knee restraints) unembalmed PMHSs were tested on a sled system, at two different velocities, utilizing a custom-made rigid seat setup. Data from experiments performed by Pintar *et al.* (2010) were used for this validation study. A detailed description of the experimental setup can be found in [18], for completeness, only a brief description is presented here. Four unembalmed PMHSs (age: 60.0±22.7; height: 169.5±7.0 cm; weight: 59.2±21.5 kg) were tested on a sled system, at low (3.3 m/s), and medium (6.7 m/s) velocities, using two input acceleration pulses. Each PMHS was tested with the low speed, followed by medium the speed pulse, resulting in a total of eight tests. Each PMHS was seated on a custom rigid seat with a seat pan at 15 degrees from the horizontal, and the seat back was 25 degrees with respect to the vertical (**Figure 1.a**). The seat was rigidly attached to a sled platform that applied the input pulses. The platform also accommodated fixtures to attach three-point seatbelt and knee restraints. The belt positioning followed FMVSS-208 testing protocol. The knee restraint assembly consisted of a plate at an angle of 45 degrees, and a paper honeycomb (205 kPa) was fixed to the plate's outer surface. The restraint was fixed in front of the lower limb, such that the distance between the limb, and the surface of the honeycomb was 25 mm.

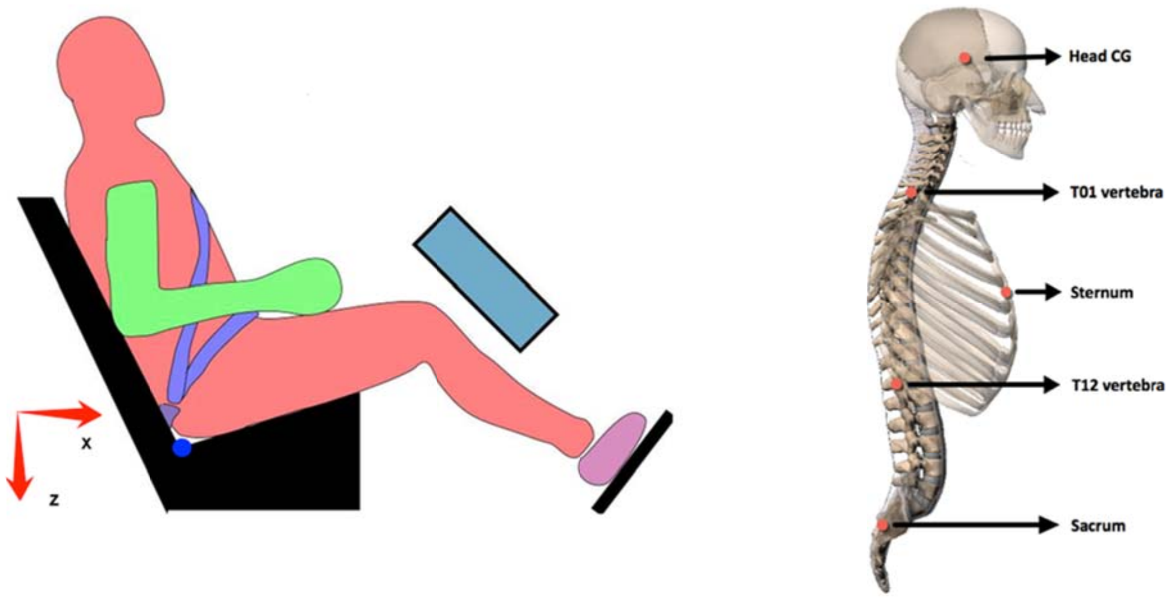

Figure 1 (a) Schematic representation of experimental setup (blue dot shows the origin of the coordinate system) (b) Anatomical locations of measured accelerations

Instrumentation and data processing:

Acceleration data – collected (using accelerometer packages) at head CG, T1, sternum, T12, and sacrum - were filtered and time-zeroed using accepted methods. A pyramid-shaped nine-accelerometer package (PNAP) was attached to the surface of the specimen's head. Using kinematic equations, data from the package were transformed to estimate accelerations at the center of gravity of the specimen's head. Using custom-made mounts, linear tri-axial accelerometer packages were attached at the T1, T12, and sacrum levels to the posterior side of the spine. In addition, a tri-axial package was attached to the sternum, between third and fourth ribs of the specimen (**Figure 1.b**). The acceleration data were filtered using the SAE CFC 60 filter standards. High-speed videos were used to capture the experiment at 1000 frames per second; frames from these videos were used to qualitatively compare the kinematics of the GHBMC. Retro reflective markers were attached to the posterior sides of the head and T1 spine, these markers were tracked using Vicon cameras at 1000 frames per second. Data from these markers were transformed to head CG and T1 vertebral body and used to compare head-T1 posture between experiments and model (see discussion).

Experimental data normalization:

The normalization procedure considered in this study used a basic approach proposed by Eppinger (1976) that assumes linear relation between length, mass, and time units [12]. Furthermore, the procedure assumes identical tissue density and elastic modulus between individual PMHS and reference PMHS. The following equations show the normalization factors for acceleration (a) and time (t). The original signals were multiplied by the normalization factors to derive the normalized signals, using the equations (1) and (2). The normalization factors used in this study are given in Table 1.

$$a_n = \lambda_a \times a_i \,; where\ \lambda_a = \lambda^{\frac{-1}{3}} \quad (1)$$

$$t_n = \lambda_t \times t_i \,; where\ \lambda_t = \lambda^{\frac{1}{3}} \quad (2)$$

Where, the subscripts n and i denote normalized and original signals. Lambda (λ) is the normalizing factor, which is given by the ratio between the reference mass (76 kg) that represent the target population, and individual PMHS mass.

Table 1 Normalization factors used for this study

	Normalizing factors	
Specimen ID	**Time (λt)**	**Acceleration (λa)**
FC133	1.088	0.919
FC197	1.307	0.765
FC220	0.958	1.044
FC237	1.099	0.910

Simulation setup:

The restrained model was placed on a rigid seat and the deceleration pulses were applied to the seat, to simulate experimental loading conditions. The GHBMC model with its standard posture was positioned on a seat. Because the seat was not expected to deform significantly, it was modeled using rigid elements. Rigid elements were also used to model a footrest, and a B-pillar where an anchor point of the seat belt was attached (**Figure 2.a**). A generic seatbelt model – made with 550 seatbelt, and 60 one-dimensional elements – was included in the setup, to mimic the experimental boundary conditions. A fabric material property was assigned to the seatbelt model to mimic real world seatbelts. From experimental high frame-rate videos, during sled deceleration, cantilever-like high magnitude vibration of knee restraint fixtures was observed; therefore the restraint did not significantly engage the lower limb. Hence, the knee restraint was not included in the simulation setup. The seat, B-pillar, and the footrest were rigidly constrained – using the *RIGID_CONSTRAINT ls-dyna keyword – to avoid relative motions between the structures. The coefficient of friction between the GHBMC model and the rigid seat was defined as 0.249 [15], to mimic the contact between neoprene and Teflon surface. At the start of the simulations, initial velocities were applied to the whole model using

*INITIAL_VELOCITY keyword, to mimic the stored kinetic energies in experimentations. Then, the deceleration sled pulses (**Figure 2.b**) were applied to the rigid seat to load the GHBMC model, mimicking sled tests. As the lower spine biofidelity was evaluated, and because the vertebral bodies in the lower spine was constructed with rigid bodies, the joint stiffness between the vertebral bodies may play a significant role in overall lower spine biofidelity. However, in the original model, joints were not defined in the lower spine. Therefore common nodes were created using *CONSTRAINED_EXTRA_NODES and spherical joints were defined, between vertebral bodies (Figure 3.a). The stiffness data of the T11-T12 joint was used for the defined joints in the lower spine. The joints were defined per SAE J211 sign convention (Figure 3.b).

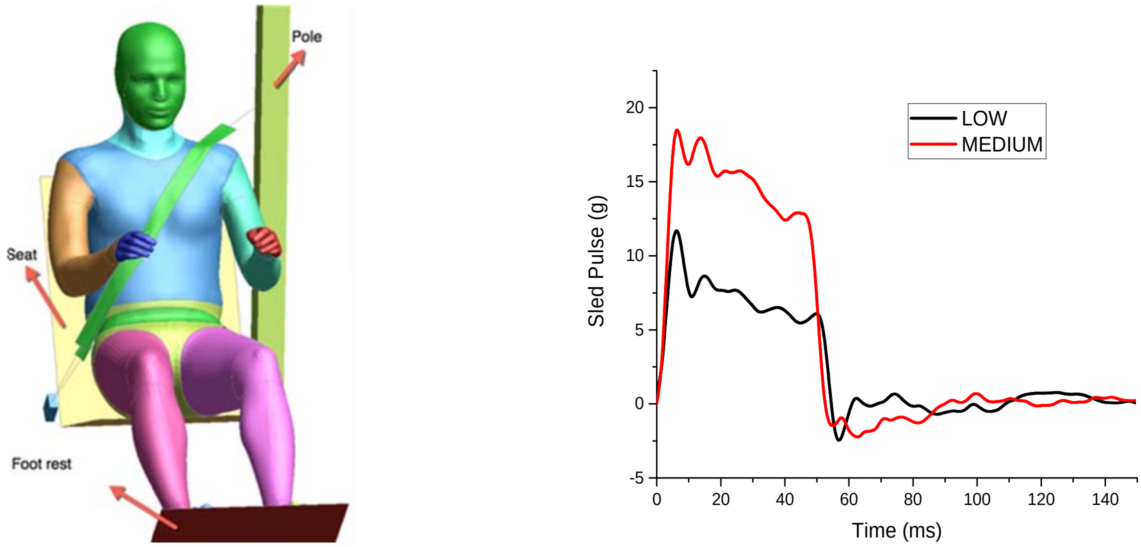

Figure 2 (a) Simulation setup (b) Input sled pulses used in this study

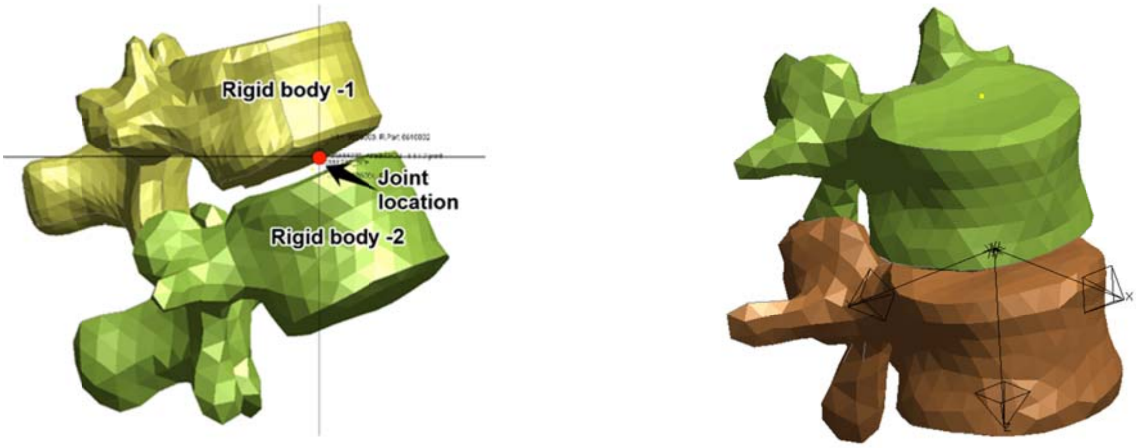

Figure 3 (a) Joint definition between rigid vertebral bodies (b) Sign convention used in joint definition

Resultant nodal acceleration data from simulation results were compared with the respective normalized experimental data. In order to compare the responses from the model, and experiments, resultant nodal accelerations from head CG, T1, sternum, T12, and sacrum from the model were extracted from respective nodes. Because the nodal acceleration data were too noisy, even after filtering, hence component wise (x, y, and z) velocity data were differentiated, and operated to obtain resultant accelerations. The calculated resultant accelerations were then compared with experimental data, using correlation methods to quantify the goodness-of-fit. In addition, it was observed that the resultant accelerations directly given by the post processing application (LS-PREPOST) were not accurate, as they were calculated internally before filtering the acceleration components. All simulations were solved using Ls-Dyna MPP version 7.0 solver on a Linux RHEL 5.4 computational cluster, using 64 cores.

Correlation analyses:

Correlation and analyses (CORA) was used to quantify the goodness-of-fit between simulation and experimental responses. The ratings in CORA range from 0 to 1, where 0 representing poor correlation, and 1 representing perfect match. CORA uses two methods – that are fundamentally very different – to quantify the degree of correlations between the responses. The first method is the corridor method that calculates the correlation between the responses using user-defined corridors. This method calculates a mean trace using individual experimental responses. Along the mean trace, two corridors – an inner, and an outer corridor – are generated with a constant y-offset. This offset is computed by the user-defined percentage of the peak mean trace. In this study, the inner corridors were calculated for 5 percent of the peak mean trace, whereas the outer corridor was calculated for 50 percent of the peak mean trace (**Figure 4**). For each time step, if the simulation response lies within the inner corridor then a rating of 1 is given, whereas if the response lies outside the outer corridor a rating of 0 is given. However, if the response lies in between the inner and the outer corridors a rating between 0 and 1 is given, based on the user defined blending function. The overall rating for the corridor method is calculated by averaging all ratings from each time step. The advantage of this method is its directness and simplicity; however, the major disadvantage of this method is that the rating could become poor if there is a time shift between the responses. A cross-correlation method is used to compensate this disadvantage posed by the corridor method.

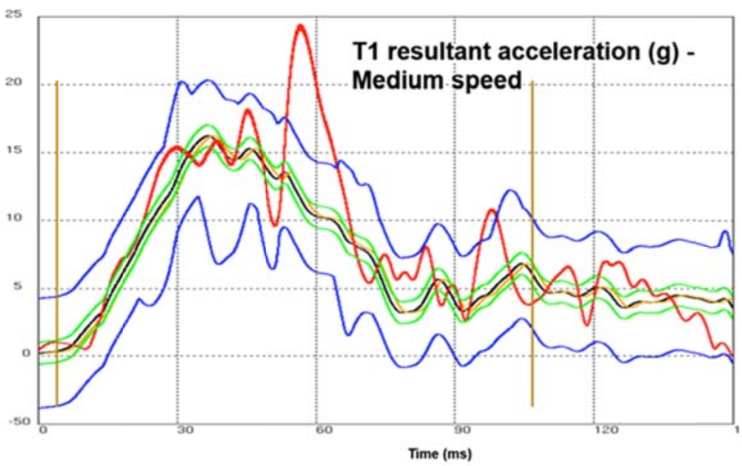

Figure 4 Corridor method: black curve shows the mean trace; red curve shows the simulation response; green curves show 5 percent (of peak mean) inner corridor; and blue curves show 50 percent outer corridor

The cross-correlation method is more involved and complex, for brevity, only a brief description is presented here, a more detailed description can be found in [19]. This method quantifies the progression, time-shift, and size of the responses, using three respective metrics (**Figure 5**). The cross correlation method starts by time-shifting the mean curve by a small time step, and a cross correlation value is calculated for each time-shifted state. All the three metrics are calculated using the time-shifted data for the maximum cross correlation value. Weighted sum of these three metrics give the rating for correlation method. Equally weighted sum of the corridor, and cross-correlation methods give the overall correlation rating. The CORA parameters used in this study are listed in Table 2. These parameters can be found and edited per need in the "*.cps" file inside the CORA execution directory.

Figure 5 Plots showing (a) progression rating (b) time-shift rating (c) size rating

Table 2 CORA parameters used in this study

Method	Parameters	Values	Description
Corridor	K	2	Transitional order of function between ratings of 1 and 0
	G_1	0.5	Weighting factor of the corridor method
	A_0	0.05	Width of the inner corridor
	B_0	0.5	Width of the outer corridor
	A_SIGMA	0	Parameter to widen the inner corridor
	B_SIGMA	0	Parameter to widen the outer corridor
Cross correlation	D_MIN	0.01	Minimum interval of evaluation
	D_MAX	0.12	Maximum interval of evaluation
	INT_MIN	0.8	Minimum interval overlap
	K_V	10	Transitional order of function between ratings of 1 and 0 for progression
	K_G	1	Transitional order of function between ratings of 1 and 0 for size
	K_P	1	Transitional order of function between ratings of 1 and 0 for phase
	G_V	0.5	Weighting factors of the progression rating
	G_G	0.25	Weighting factors of the size rating
	G_P	0.25	Weighting factors of the phase shift rating
	G_2	0.5	Weighting factors of the cross correlation method

III. RESULTS

Kinematics comparison:

Each simulation took approximately 20 hours to solve on the cluster. **Figure 6** and **Figure 7** show qualitative kinematics comparison between the experiment and simulation for the low and medium speed cases respectively, overall, the kinematics showed good agreement. In simulations, when the rigid seat started to decelerate, due the initial kinetic energy stored in the human body model, it moved forward engaging the seatbelt, hence loading the model. In both low and medium speed experiments, and simulations, the human body model changed directions and rebounded back to the seats at approximately 75 and 60 ms. The rotations of the PMHS about the z-axis due to shoulder belt engagement were also captured in simulations.

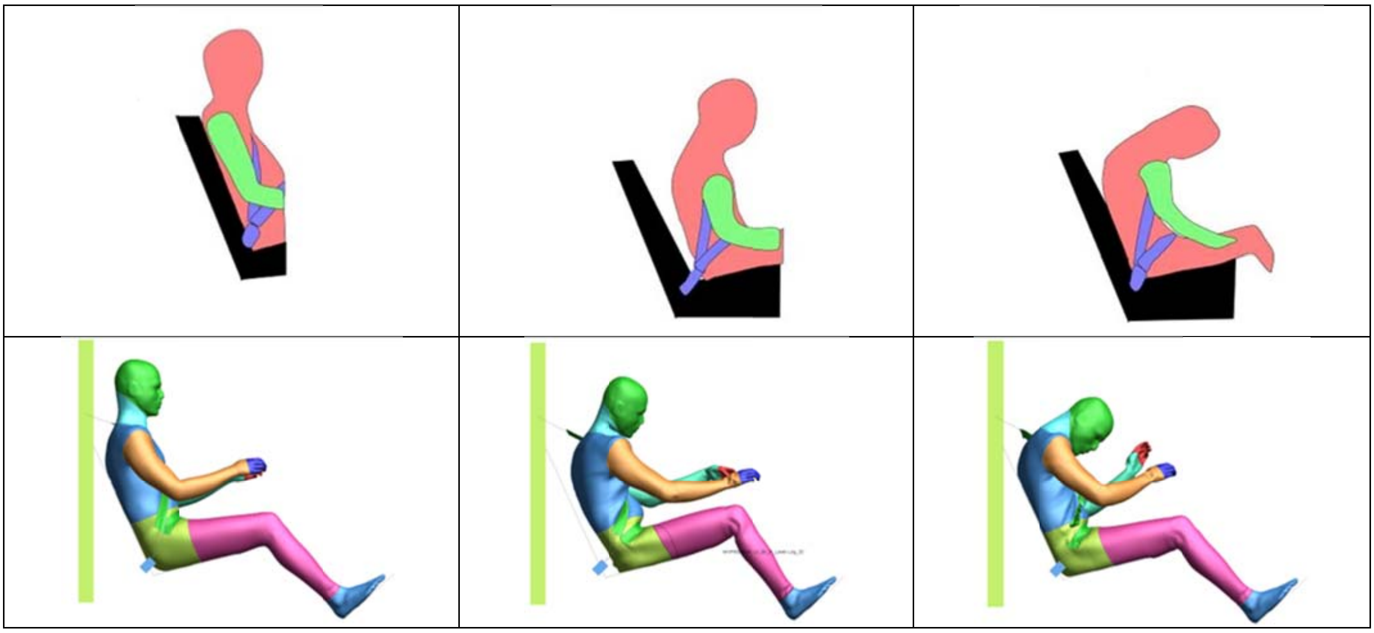

Figure 6 Motion comparison at low speed: Top row: Silhouette rendering of motion captured by high-speed video, and bottom row: motion obtained from simulation at (a) t=0 (b) t=75, and t=135 ms

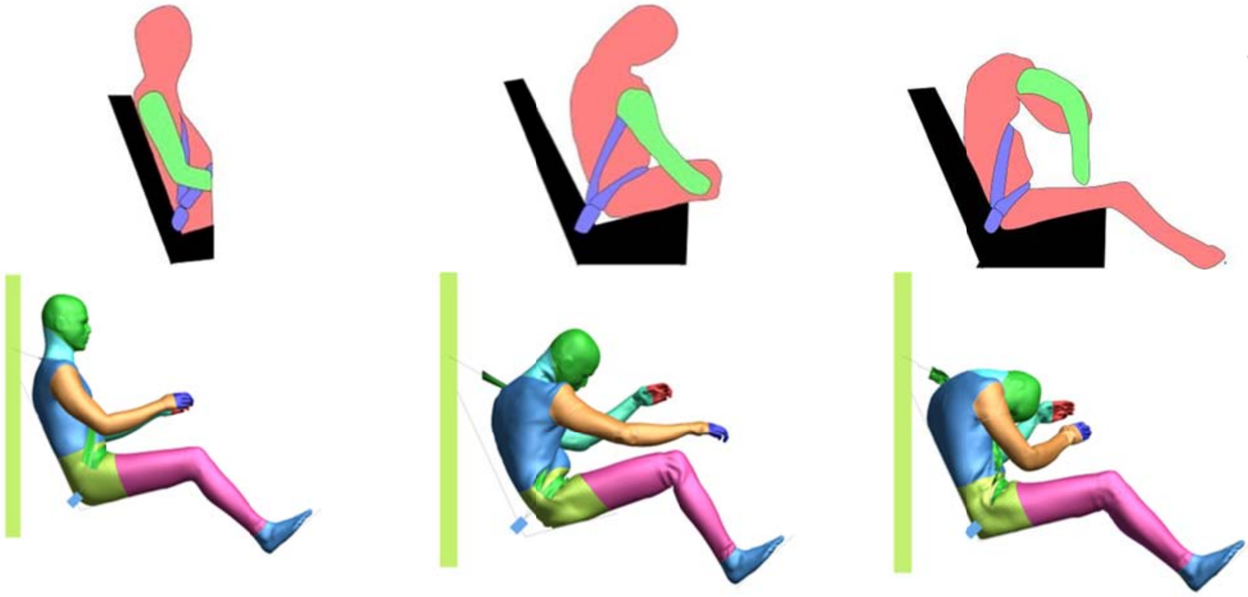

Figure 7 Motion comparison at medium speed: Top row: Silhouette rendering of motion captured by high-speed video, and bottom row: motion obtained from simulation at (a) t=0 (b) t=75, and t=135 ms

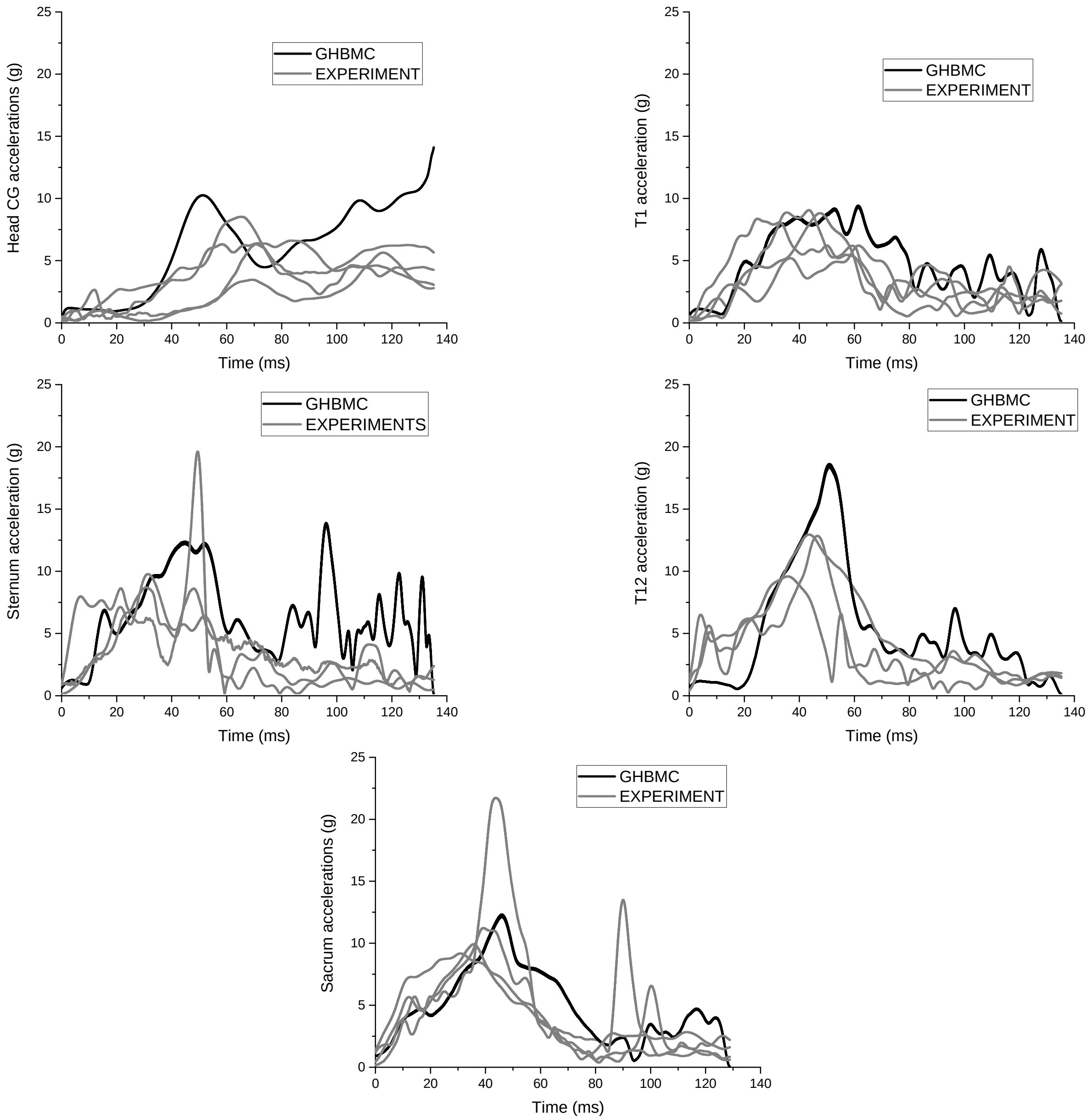

Figure 8 Normalized resultant acceleration data from experiments, and simulation for low speed case

Data Normalization:

The normalized low, and medium speed data are presented in **Figure 8** and **Figure 9**. For low, and medium speed cases, experimental peak head CG accelerations ranged from 3 to 9, and 16 to 27 g, whereas the simulations showed approximately 10 and 23 g. Normalized experimental T1 accelerations ranged from 6 to 9, and 18 to 20 g, whereas for simulations the accelerations were 9 and 25 g. For sternum the experimental accelerations were between 9 and 20, and 16 and 23 g, although simulations showed 14 and 31 g. Experimental T12 accelerations indicated a range from 10 to 13, and 19 to 26 g, whereas simulations indicated 19 and 42 g. Finally, for sacrum the experimental accelerations were between 9 and 22, and 20 and 35 g, with simulations indicating 12 and 26 g. Also it should be noted that the PMHS did not show stiffness degradation after low speed tests, therefore the response of the medium speed tests were not affected by low speed tests, more information on this can be found in Pintar *et al.* (2010).

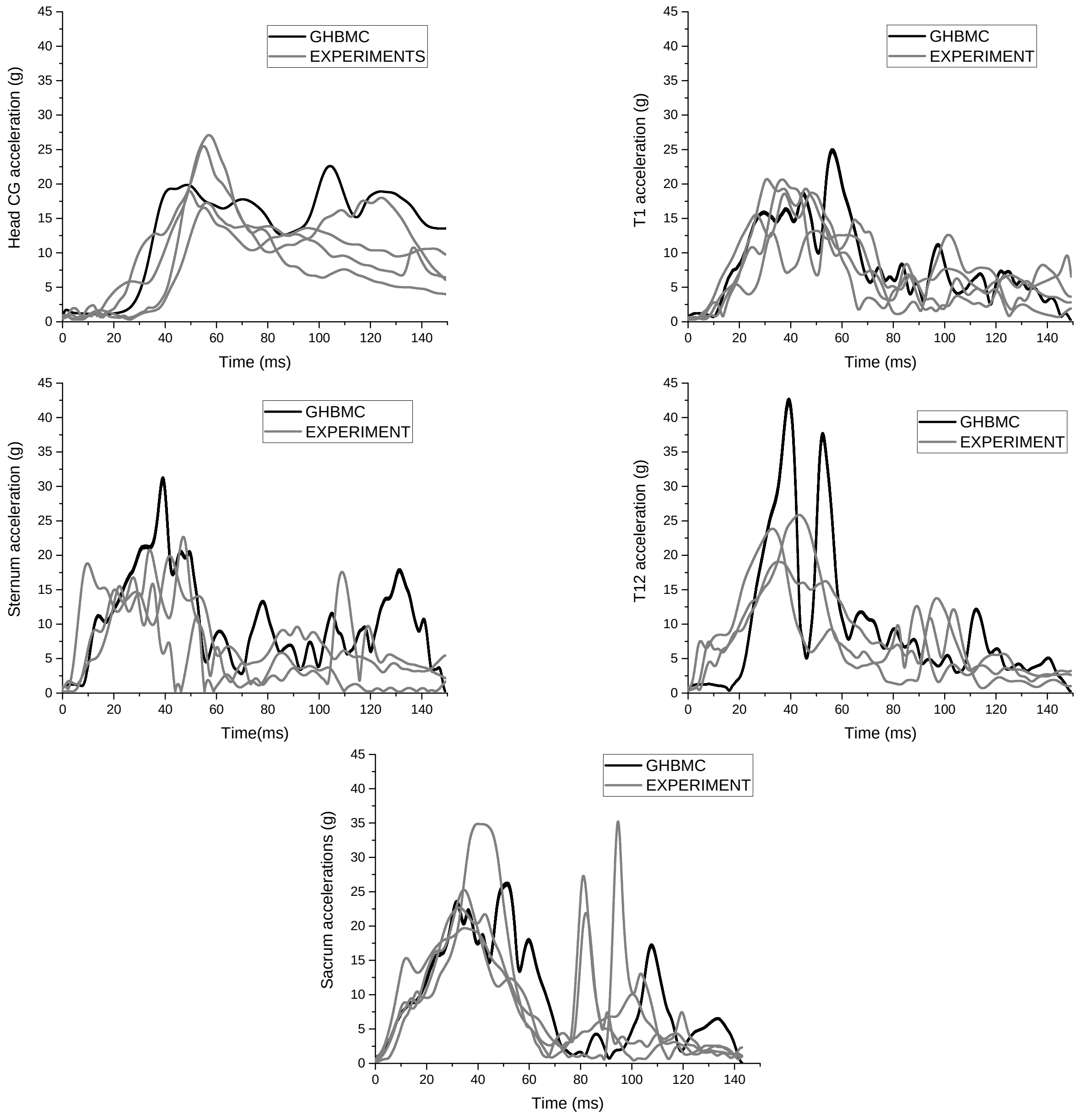

Figure 9 Normalized resultant acceleration data from experiments, and simulation for medium speed case

Correlation analyses:

The results from the correlation analyses are shown in **Table 3**. For the low, and medium speed cases, the combined rating was highest for the sacrum, whereas the lowest rating was to the head CG, and T12 respectively. It was interesting to observe the increasing trend in average corridor, and combined ratings, as the speed increased.

Table 3 CORA ratings for different body regions

Speed	Region	Corridor Method	Cross correlation	Combined rating
Low	Head CG	0.445	0.563	0.504
	T1	0.442	0.840	0.641
	Sternum	0.501	0.731	0.616
	T12	0.352	0.685	0.519
	Sacrum	0.685	0.869	0.777
Average:		**0.485**	**0.738**	**0.611**
Medium	Head CG	0.612	0.739	0.676
	T1	0.685	0.815	0.750
	Sternum	0.503	0.691	0.597
	T12	0.433	0.632	0.533
	Sacrum	0.600	0.795	0.697
Average:		**0.567**	**0.734**	**0.651**

IV. DISCUSSION

The objective of the present study was to evaluate the biofidelity of the restrained GHBMC model by comparing its kinematics to that of PMHS sled tests, under frontal impact. Resultant acceleration data at head CG, T1, sternum, T12, and sacrum from eight PMHS tests – four low, and four medium speeds – were compared with nodal acceleration data from the GHBMC model. The experimental data were normalized to minimize effects due to variations in demographics. To quantify the goodness-of-fit between the simulation, and experimental responses, correlation analyses were performed using CORA methodology. It should be noted that the resultant nodal accelerations were obtained by differentiating and operating on component velocities. This process was verified using trial problems with know accelerations and velocities, therefore, this process was not expected to introduce significant errors in the model responses.

When the kinematics between the experiments and simulations were qualitatively compared, the overall response showed a good agreement. In experiments, because the seatbelt was anchored to the left-hand side of the PMHS, and when the shoulder belt loaded the specimen, it rotated in the counter-clock direction with respect to the z- axis. The GHBMC model also captured this complex motion. The initial posture of the PMHS may have influenced the response corridors, and in turn the biofidelity ratings of the model. The posture of the GHBMC model was derived using a 26-year-old (young) living subject; however, this kind of ideal posture may not be obtained during PMHS testing mainly due to the age of the PMHS, absence of muscle activity, forceful artificial boundary conditions, and availability of test specimens. In order to give a quantified idea of the difference in initial posture between the PMHS and GHBMC, two extreme cases were presented in **Figure 12** and **Figure 13**. Head and T1 coordinates were considered in this comparison as retro reflective trackers were used only at these two regions in the tests. **Figure 12** shows the case in which the postures – between head CoG and T1 - had minimum difference and **Figure 13** shows the case in which the postures had maximum difference, out of the considered 8 test cases. Despite these variations in initial posture, correlation analyses for the acceleration data showed ratings of 0.5 and 0.7 for head under low and medium speed impact respectively; and 0.6 and 0.8 for T1 under low and medium speed impact respectively. However, performing experiments with initial posture similar to the ideal GHBMC posture may have resulted in a mean curve closer to the model's response somewhat improving biofidelity ratings.

Kinematics validation of the whole body GHBMC model was not reported in literature for frontal impacts; however, Park *et al.* (2013) evaluated the biofidelity of the model using kinematic data from lateral impact sled tests and used CORA to rate the good-of-fit [15]. Using an impact velocity of 4.3 m/s, they compared accelerations of the model at T1, T6, and pelvis with experimental responses, and the CORA ratings were reported as 0.27, 0.37, and 0.68 respectively. However, it is not clear whether the reported CORA ratings were using the corridor method or correlation method, or the weighted sum of both the methods.

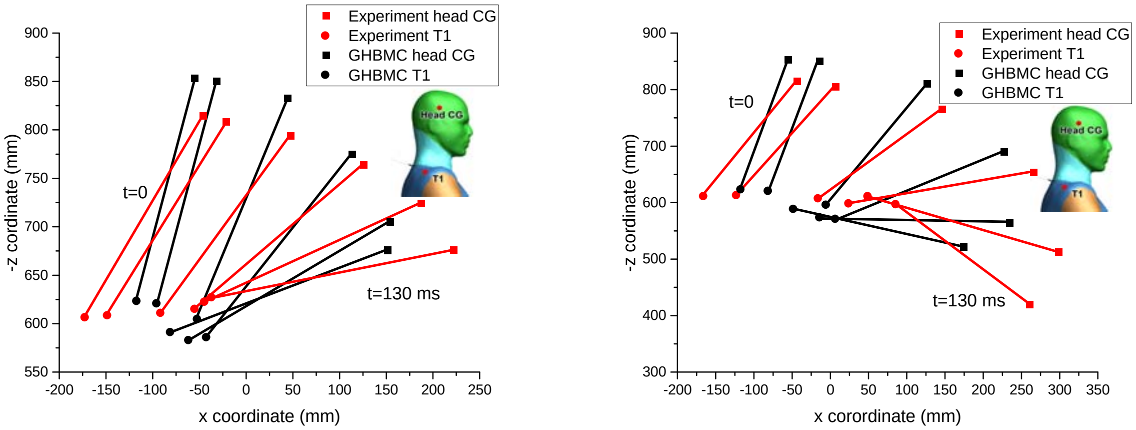

Figure 10 Head CoG and T1 posture with minimum difference for (a) low speed, and (b) medium speed

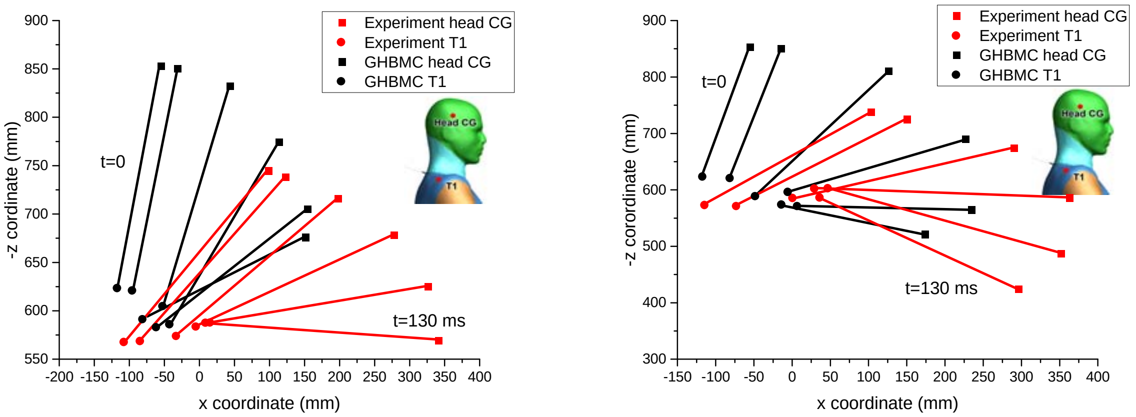

Figure 11 Head CoG and T1 posture with maximum difference for (a) low speed, and (b) medium speed

As indicated in the methods section, in the present study, for CORA ratings with the corridor method, 50% of the peak mean values were used to construct the outer corridor. However, the ratings – both corridor, and overall rating - could differ if the width of the outer corridor is varied. In order to observe the difference, the ratings were calculated for corridors constructed using 25% of the peak mean values. **Figure 12** and **Figure 13** shows the comparison of corridor, and overall ratings between 50%, and 25% outer corridors for low, and medium speeds. In the corridor ratings the highest variations were observed in T12, in which the ratings between 50, and 25 percent outer corridors dropped by 48, and 43 percent, for low, and medium speeds. However, due to the contribution from the correlation method, for T12 the overall ratings only dropped by 16, and 18 percent, for low and medium speeds. Therefore these construction parameters in CORA should be chosen appropriately depending on specific requirements, and applications.

One of the limitations of the present study is the usage of a generic seatbelt material property, instead of a characterized material property, used in the specific experimental sled tests. Considering the high stiffness of these seatbelt materials, using a generic model should not make a significant difference, however minimum variations could occur in simulation responses. The other limitation is the vertebral bodies of the thoracic, and lower spine were modeled using rigid body elements, and the intervertebral discs were constructed using a beam element surrounded by shell elements. Though these types of constructions may only estimate the real world kinematics, and kinetics of the lower spine. In order to closely approximate the motions and loads, a more realistic deformable model is preferred over rigid bodies, hence may further increase the GHBMC model's correlation ratings.

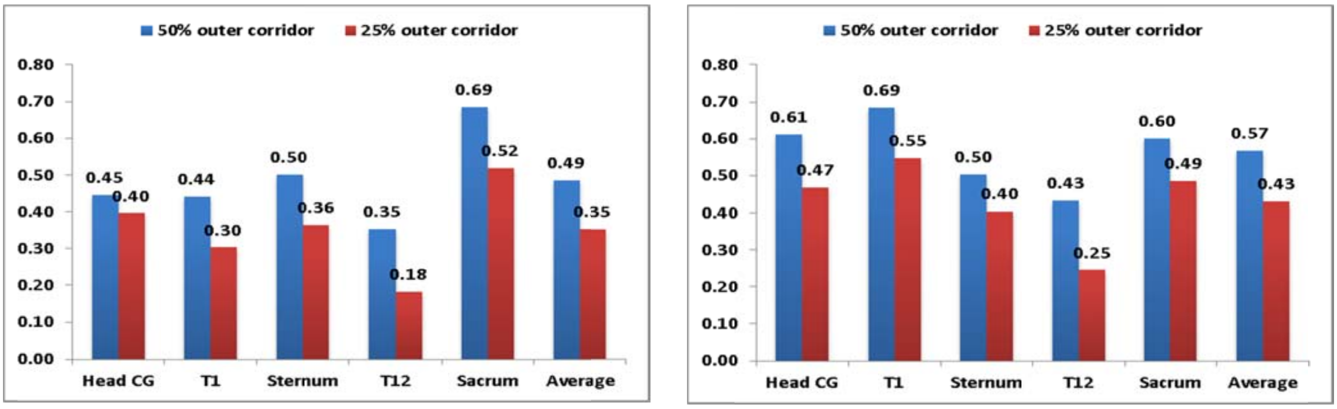

Figure 12 Comparison of corridor ratings between 50%, and 25% outer corridors for (a) low speed (b) Medium speed

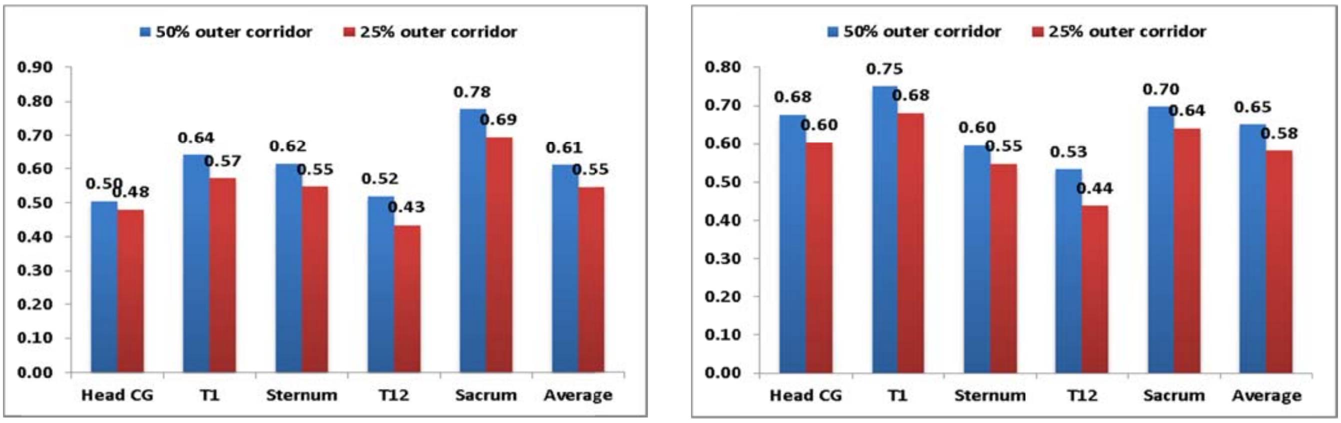

Figure 13 Comparison of overall ratings between 50%, and 25% outer corridors for (a) low speed (b) Medium speed

V. CONCLUSIONS

This study evaluated the biofidelity of the GHBMC finite element model, using normalized kinematic data from eight sled tests with two different speeds, under frontal impact condition. Qualitative observation of the kinematics between simulations and experiments showed a good match. Combined CORA ratings ranged from 0.51 to 0.78, and 0.53 to 0.75 for the low, and medium speed cases, indicating acceptable kinematics biofidelity of the model under frontal impact.

VI. ACKNOWLEDGEMENT

The study was supported by the US Department of Transportation DTNH22-13-D-00290. This material is the result of work supported with resources and the use of facilities at the Zablocki VA Medical Center, Milwaukee, Wisconsin and the Medical College of Wisconsin. The authors would like to thank the Global Human Body Model Consortium for providing the model for this study. The authors would also like to thank Argonne National Laboratory for providing cluster resources. The authors thank Dr. Rodney Rudd from NHTSA for his feedback on this manuscript. Any views expressed in this article are those of the authors and not necessarily representative of the funding organizations.

VII. REFERENCES

1. Lopez-Valdes, F.J., P.O. Riley, D.J. Lessley, K.B. Arbogast, T. Seacrist, S. Balasubramanian, M. Maltese, and R. Kent, *The six degrees of freedom motion of the human head, spine, and pelvis in a frontal impact.* Traffic Inj Prev, 2014. **15**(3): p. 294-301.

2. Yoganandan, N., M.W. Arun, D.E. Halloway, F.A. Pintar, D.J. Maiman, A. Szabo, and R.W. Rudd, *Crash characteristics and injury patterns of restrained front seat occupants in far-side impacts.* Traffic Inj Prev, 2014. **15 Suppl 1**: p. S27-34.
3. Yang, K.H., J. Hu, N.A. White, A.I. King, C.C. Chou, and P. Prasad, *Development of numerical models for injury biomechanics research: a review of 50 years of publications in the Stapp Car Crash Conference.* Stapp Car Crash J, 2006. **50**: p. 429-90.
4. Klinich, K.D., M.P. Reed, M.A. Manary, and N.R. Orton, *Development and testing of a more realistic pelvis for the Hybrid III 6-year-old ATD.* Traffic Inj Prev, 2010. **11**(6): p. 606-12.
5. Newby, N., J.T. Somers, E.E. Caldwell, C. Perry, J. Littell, and M. Gernhardt, *Assessing biofidelity of the Test Device for Human Occupant Restraint (THOR) against historic human volunteer data.* Stapp Car Crash J, 2013. **57**: p. 469-505.
6. McHenry, *Analysis of the dynamics of automobile passenger restraint system*, in *Proc of 7th Stapp Car Crash Conference*. 1963. p. 207-249.
7. Schinkel-Ivy, A., W.J. Altenhof, and D.M. Andrews, *Validation of a full body finite element model (THUMS) for running-type impacts to the lower extremity.* Comput Methods Biomech Biomed Engin, 2014. **17**(2): p. 137-48.
8. Sun, J., A. Rojas, P. Bertrand, Y. Petit, R. Kraenzler, and P.J. Arnoux, *Investigation of motorcyclist cervical spine trauma using HUMOS model.* Traffic Inj Prev, 2012. **13**(5): p. 519-28.
9. Bathe, K.-J., *Finite element procedures*. 1996, London: Prentice Hall.
10. Hallquist, J.O., *LS-Dyna theory manual*. 2006: Livermore software technology corporation.
11. Yoganandan, N., M.W. Arun, and F.A. Pintar, *Normalizing and scaling of data to derive human response corridors from impact tests.* J Biomech, 2014. **47**(8): p. 1749-56.
12. Eppinger, R.H. *Prediction of thoracic injury using measurable experimental parameters*. in *Proceedings of the International Conference of Experimental Safety Vehicles, NHTSA, Washington, DC*. 1976.
13. Mertz, H.J., *A procedure for normalizing impact response data*. 1984, SAE Technical Paper.
14. Moorhouse, K. *An improved normalization methodology for developing mean human response curves*. in *Proceedings of the International Conference of Enhanced Safety of Vehicles, Seoul, Korea, Paper*. 2013.
15. Park, G., T. Kim, J.R. Crandall, C. Arregui-Dalmases, and J. Luzon-Narro, *Comparison of Kinematics of GHBMC to PMHS on the Side Impact Condition*, in *IRCOBI*. 2013: Gothenburg.
16. Hayes, A.R., N.A. Vavalle, D.P. Moreno, J.D. Stitzel, and F.S. Gayzik, *Validation of simulated chestband data in frontal and lateral loading using a human body finite element model.* Traffic Inj Prev, 2014. **15**(2): p. 181-6.
17. Vavalle, N.A., M.L. Davis, J.D. Stitzel, and F.S. Gayzik, *Quantitative Validation of a Human Body Finite Element Model Using Rigid Body Impacts.* Ann Biomed Eng, 2015.
18. Pintar, F.A., N. Yoganandan, and D.J. Maiman, *Lower cervical spine loading in frontal sled tests using inverse dynamics: potential applications for lower neck injury criteria.* Stapp Car Crash J, 2010. **54**: p. 133-66.
19. Gehre, C., H. Gades, and P. Wernicke. *Objective rating of signals using test and simulation responses*. in *21st International Technical Conference on the Enhanced Safety of Vehicles, Stuttgart, Germany*. 2009.